Expanding the Field Range of PHE Sensors for Increased Industrial Applicability

Department of Physics, Faculty of Exact Sciences, Bar-Ilan University

BINA Bar-Ilan Institute of Nanotechnology & Advanced Materials, Bar-Ilan University

Daniel Lahav[1], Moty Schultz[1], Shai Amrusi[2], Asaf Grosz[2] and Lior Klein[1]

[1]Department of Physics, Institute of Nanotechnology and Advanced Materials, Bar-Ilan University, Ramat-Gan 52900, Israel

[2]Department of Electrical and Computer Engineering, Ben-Gurion University of the Negev, P.O. Box 653, Beer-Sheva 84105, Israel

Motivation - The Need for Range

- Magnetic field sensing plays a pivotal role in **numerous technological** applications, including automotive, biomedical diagnostics and more.
- Planar Hall effect (PHE) sensors provide **superior performance**, **simpler fabrication**, **high resolution**, and **low temperature dependence** compared to other sensors.
- The field range of high-resolution PHE sensors is typically limited to hundreds of micro-Tesla, restricting their applicability in certain critical areas.

- **Extending the field range of PHE sensors is essential** to meet the demand for measuring a wide range of field strengths in industrial, scientific, and consumer applications.
- This extension **enhances applicability** while **requiring careful evaluation** of its impact on performance metrics, such as equivalent magnetic noise (EMN), to optimize sensor performance.

Fabrication Process

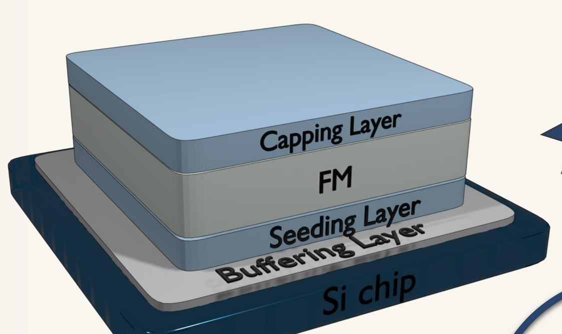

(i) Ion beam sputtering.

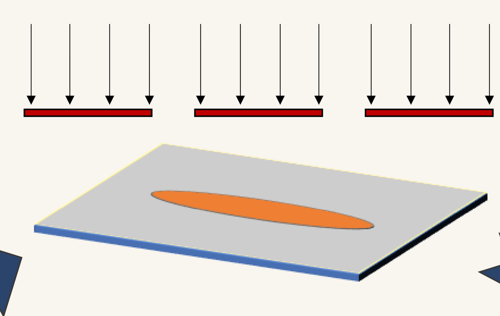

(ii) First photolithography.

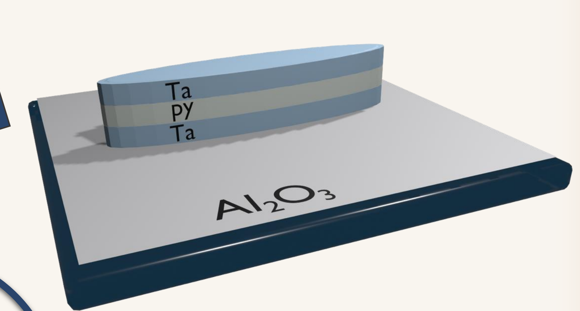

(iii) Sensor layer stack after first lift-off process.

(i) A stack comprising Al_2O_3(35nm)/Ta(15nm)/ Py(200nm)/Ta (15nm) is being deposited onto a wafer using an Ion Beam Sputtering (IBS) system.

(ii) Photolithography is employed to create elliptical shapes.

(iii) The first lift-off process is utilized to reveal the elliptical shape.

(iv) Gold electrical contacts are deposited using the IBS and created through photolithography.

(v) The second lift-off process is employed to reveal the gold contacts.

(vi) Cleaning and cutting the wafer to get the final EPHE sensor.

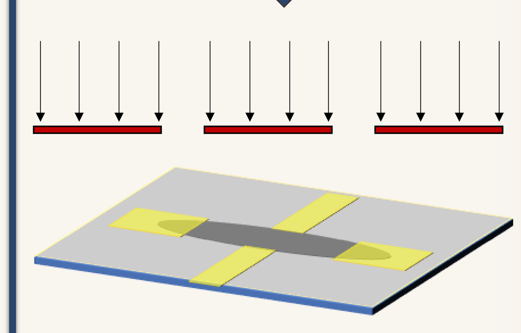

(iv) Au deposition using BesTec and Photolithography using MLA150.

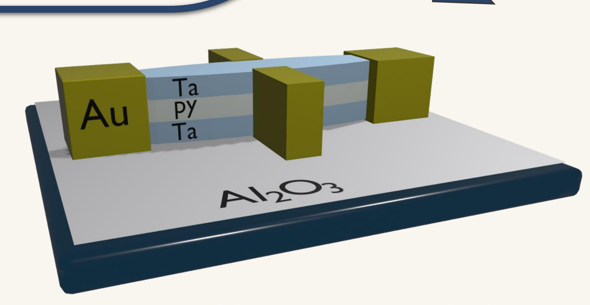

(v) Sensor layer stack after second lift-off process.

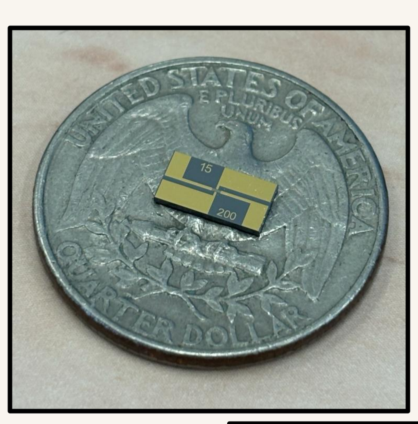

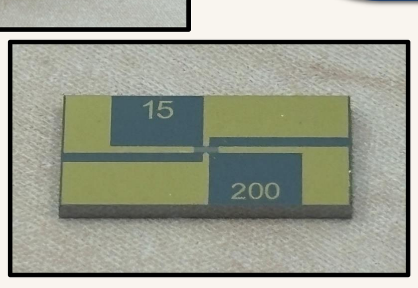

(vi) EPHE sensor after cleaning and cutting the wafer.

Results

Table 1 demonstrates that reducing the hard axis dimension (b) while maintaining the a/b ratio extends the field range of the EPHE sensor. At a constant current density, the 20-micron sensor's sensitivity is approximately 100 times lower than the 200-micron sensor, in close agreement with theoretical predictions.

b (μm)	I (mA)	$H_{\rm eff}$ (Oe)	S_y (mV/T)	$\Delta R_{\rm PHE}$ (mΩ)	R_x (Ω)	R_y (Ω)
20	3	124.8	7.2	29	8.9	35.6
50	7.5	43.5	46	26	7	20.7
100	15	23.8	151.5	25	5.6	14.4
200	30	13.5	642.1	26	5.1	9.8

Table 1. Typical values of $H_{\rm eff}$, S_y, $\Delta R_{\rm PHE}$, R_x, and R_y for EPHE sensors with varying hard axis lengths, while maintaining uniform current density.

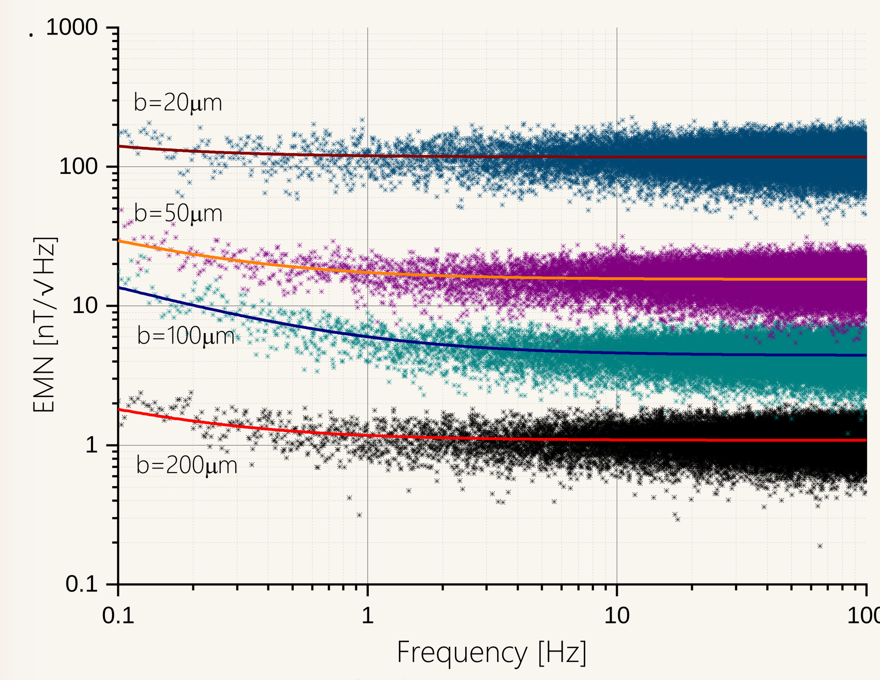

Figure 1. Equivalent magnetic noise (EMN) of the PHE sensors versus frequency for different hard axis (b) values, with the same current density.

Figure 1 shows the EMN from 0.1 to 100 Hz for sensors with varying hard axis values. The EMN is fitted using $\mathrm{EMN}(f) = \sqrt{B^2 + \frac{A^2}{f}}$, where A and B are fitting parameters. At 10 Hz, the EMNs are approximately 1.1, 4.4, 16, and 117 $^{nT}/_{\sqrt{Hz}}$ for hard axis values of 200, 100, 50, and 20 microns, respectively. The results demonstrate that the EMN scales roughly as n^2, with the 20-micron sensor having an EMN about 100 times larger than the 200-micron sensor, as predicted.

Notably, doubling the current density results in EMNs of 56 $^{nT}/_{\sqrt{Hz}}$ and 7.7 $^{nT}/_{\sqrt{Hz}}$ at 10 Hz for the 20-micron and 50-micron sensors, respectively.

Figure 2 shows the extended field range of the sensors in response to a magnetic field along the hard axis. The resistivity was measured during both ascending and descending fields and compared to the theoretical fit from the Stoner–Wohlfarth (SW) model:

$$R_{\rm PHE} = \frac{\Delta R_{\rm PHE}}{H_{\rm eff}} \cdot H \sqrt{1 - \left(\frac{H}{H_{\rm eff}}\right)^2}$$

The inset presents the scaled data with normalized values $R^*_{\rm PHE} = \frac{R_{\rm PHE}}{\Delta R_{\rm PHE}}$ and $H^* = \frac{H}{H_{\rm eff}}$.

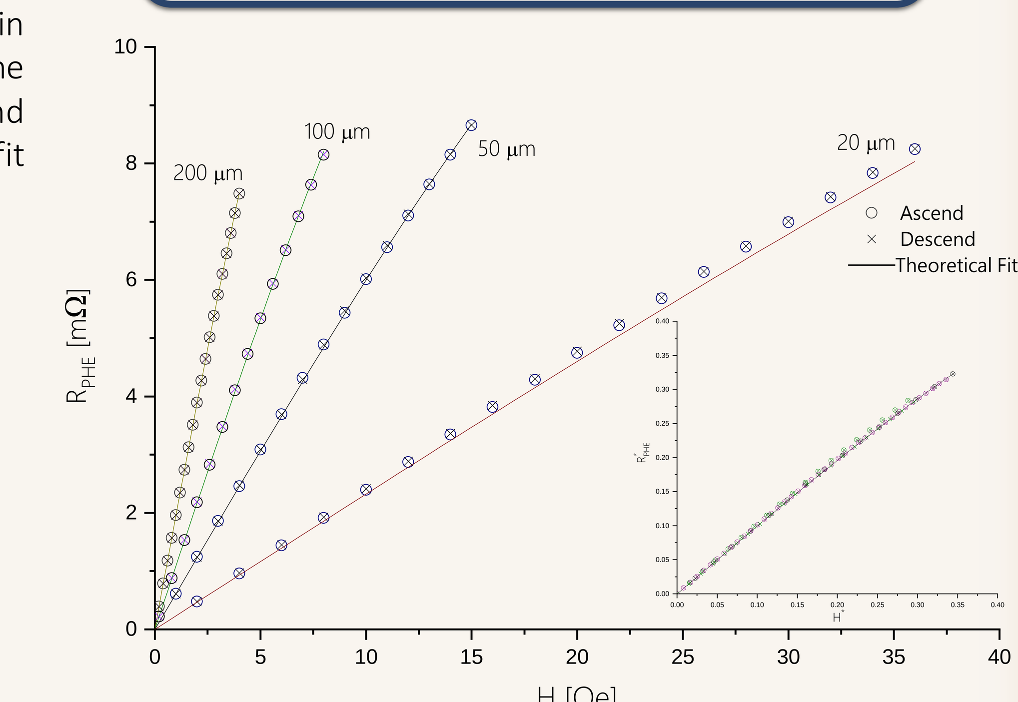

Figure 2. Operational field range of sensors with varying hard axis values.

It is evident that although all sensors exhibit non-linear behavior, this behavior can be precisely modeled, which means that they effectively behave as single magnetic domains.

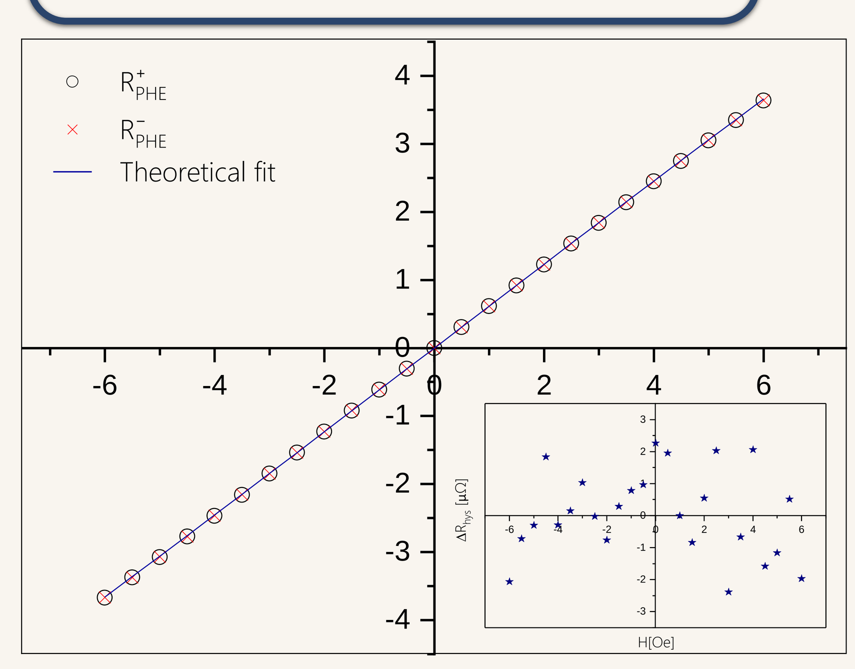

Figure 3. $R^+_{\rm PHE}$ and $R^-_{\rm PHE}$ vs. applied field parallel to the hard axis for a sensor with b = 50 microns. The inset shows the difference in resistivity values when the field is decreased from 14 Oe compared to when it is increased from −14 Oe for the same sensor.

To assess the hysteresis of a sensor with b = 50 microns, we measured $R_{\rm PHE}$ in a field range from -6 Oe to +6 Oe, where deviation from linearity is less than 1%. Using 0.5 Oe steps, $R_{\rm PHE}$ was measured twice: first reducing the field from +14 Oe and then increasing it from -14 Oe. $R^+_{\rm PHE}$ and $R^-_{\rm PHE}$ represent the averages. Figure 3 shows $R^+_{\rm PHE}$ and $R^-_{\rm PHE}$, while the inset presents the difference, $\Delta R_{\rm hys} = R^+_{\rm PHE} - R^-_{\rm PHE}$.

Significantly, $\Delta R_{\rm hys}$ changes sign, indicating that the differences are largely unrelated to magnetic hysteresis. Nevertheless, $\Delta R_{\rm hys}$ can still be considered an upper bound for any potential magnetic hysteresis.

Principle and Design

Planar Hall Effect (PHE)

Ferromagnetic materials exhibit a phenomenon called anisotropic magnetoresistance (AMR), in which their resistance changes depending on the orientation of their magnetization (**M**) relative to the direction of an applied electric current density (**J**). This phenomenon gives rise to a transverse voltage as a function of the angle θ between **M** and **J**. This effect is called PHE as the magnetization, the electric current, and the transverse electric field are in the same plane.

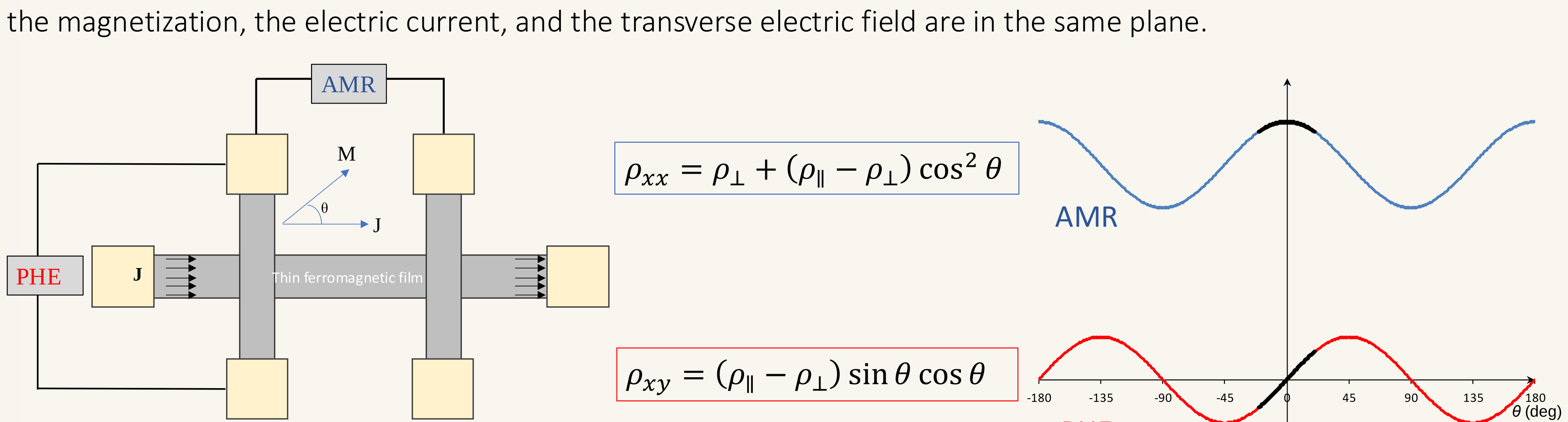

Sensitivity

The sensitivity (S_y) of an EPHE sensor is the ratio of its PHE voltage (V_y) to the applied magnetic field in the y direction (H_y), for a given current I_x along the easy axis. When H_y is small relative to the effective anisotropy field ($H_{\rm eff}$), the sensitivity is given by

$$S_y = \frac{V_y}{H_y} = I_x \frac{\Delta\rho}{\rm t} \frac{1}{H_s + H_g} = I_x \frac{\Delta\rho}{\rm t} \frac{1}{H_{\rm eff}}$$

Excitation current; Sensor thickness; Growth anisotropy; Resistivity anisotropy $\Delta\rho = (\rho_\parallel - \rho_\perp)$; Shape anisotropy

Equivalent Magnetic Noise (EMN)

The total noise, e_Σ, has three main components: 1/f noise, thermal noise, and preamplifier noise.

$$e_\Sigma(f) = \sqrt{e_{1/f}^2 + e_T^2 + e_{\rm amp}^2}$$

The sensor EMN is defined as

$$\mathrm{EMN}(f) = \frac{e_\Sigma(f)}{S_y} = \frac{\sqrt{e_{1/f}^2 + e_T^2 + e_{\rm amp}^2}}{I_x \frac{\Delta\rho}{\rm t} \frac{1}{H_{\rm eff}}}$$

A Novel EPHE Sensor with Extended Field Range

The shape of the elliptical PHE (EPHE) sensors induces a uniaxial magnetic anisotropy parallel to the long axis (the easy axis), known as “shape anisotropy”.

For an elongated and relatively flat ellipsoid (thickness t) with principal axes a and b ($a \gg b \gg t$) will be:

$$H_s \sim 4\pi M_s \frac{t}{b} \sim 10807 \frac{t}{b}$$

Utilizing this relation, we computed theoretical values of the shape anisotropy field for a sensor featuring a thickness of 200 nm across various hard axis lengths.

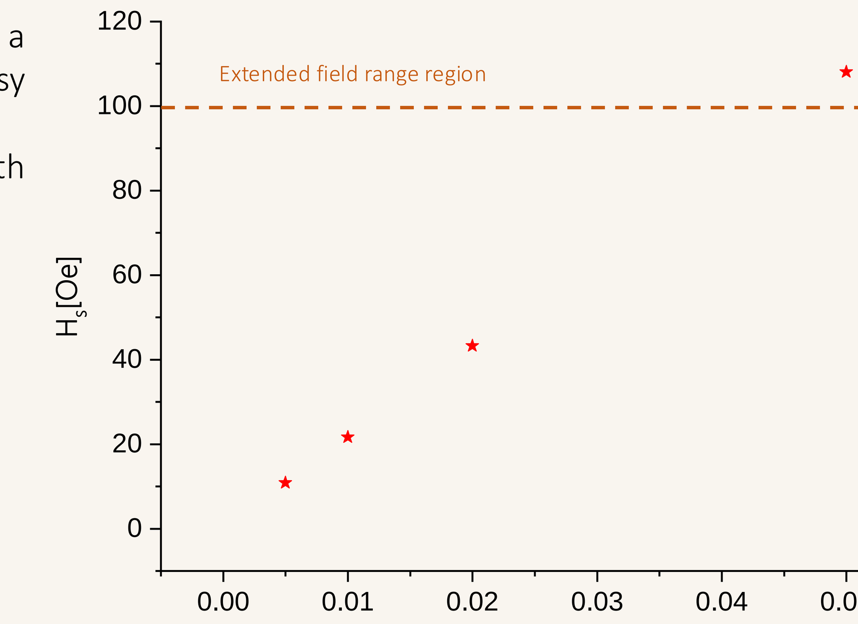

A sensor with a hard axis length of 20 microns surpasses 100 Oe, qualifying it as an extended field range sensor.

Design

We fabricate EPHE sensors with a thickness of 200 nm and hard axis lengths of 200, 100, 50, and 20 microns.

A schematic diagram of the sensor with the ellipse's major and minor axes (denoted as a and b, respectively), with aspect ratio 1:8, and the placement of the gold electrical contact pads (highlighted in yellow).

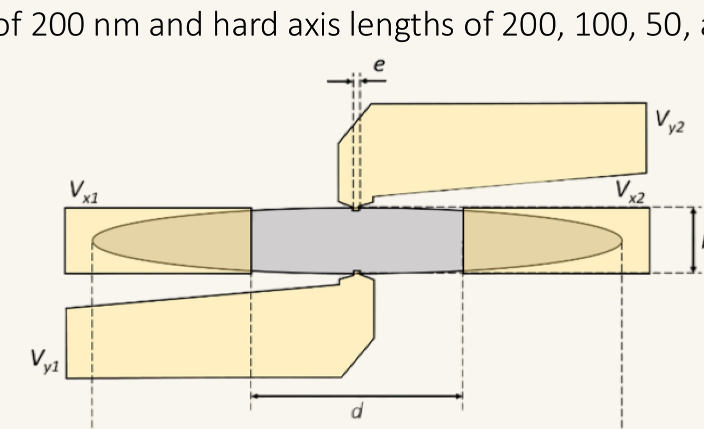

The sensor is excited by applying an ac current between V_{x1} and V_{x2}. The signal is measured between V_{y1} and V_{y2}.